Simulation of hot standby mode for flexible steam turbine operation in combined cycle power plants

Henriette Garmatter, Erik Marks, Yevgen Kostenko, David Veltmann and Roland Scharf

Kurzfassung

Simulation des Hot-Standby-Betriebs für einen flexiblen Betrieb von Dampfturbinen in Kombikraftwerken

Die Betriebsregime konventioneller Kraftwerke sind aufgrund des steigenden Anteils der erneuerbaren Energien im Energiesystem ungleichmäßiger und flexibler. Dies kann zu längeren Zeiträumen ohne Einsatzplanung für Anlagen und damit zu längeren Hochfahrzeiten des Kraftwerks nach Stillstand führen. Das Hot-Standby-Mode Konzept trägt zu einem flexibleren Dampfturbinenbetrieb bei. Es wird durch ein elektrisches Begleitheizungs-System am Gehäuse der Dampfturbine umgesetzt, das Anfahrbedingungen der Turbine hinsichtlich der Temperatur gewährleistet, wir direkt nach dem Abfahren der Turbine.

Der Wärmetransport durch die Turbine wurde untersucht, wobei der Schwerpunkt auf den Auswirkungen der Komplexität der Topologie liegt. Für die Analyse wurden drei Finite-Elemente-Modelle der Turbine eingesetzt. Alle Modelle wurden durch besondere experimentelle Messungen in Anlagen verifiziert. Numerische und experimentelle Ergebnisse zeigen eine gute Korrelation und den Nachweis, dass die Simulationen geeignet sind, alle Betriebsphasen zu erfassen. Das am besten geeignete Finite-Elemente-Modell wurde um das Trace-Heating-System erweitert. Eine Anwendung des Hot-Standby-Modus zur Temperaturhaltung der Turbine liefert Informationen über die Systemleistung. Diese zeigt, dass die Anlaufbedingungen der Turbine durch das das Trace-Heating-System deutlich verbessert werden.

Authors

Henriette Garmatter, M. Eng.
Erik Marks, M. Sc.
Leibniz Universität Hannover
Hannover, Germany

Dr.-Ing. Yevgen Kostenko
Research and Development

M. Sc. David Veltmann
Research and Development
Siemens Energy
Mülheim an der Ruhr, Germany

Prof. Dr.-Ing. Roland Scharf
Leibniz Universität Hannover
Hannover, Germany

Introduction

A continuously growing renewable power generation during advantageous weather conditions is leading to periods without any dispatch for large scale conventional power plants. They can last several days or even weeks. The consequences of these extended shut-downs are longer power plant start-up times and moderate power ramp-up due to the low metal temperatures of the steam turbine [1]. Flexible operating profiles of the fossil power plants, however, are required to react to fluctuating power requirements. To answer this demand of high flexibility in most fossil power plants, Siemens AG developed a new feature Hot Standby Mode (HSM). This feature enables a more efficient operation of the power plant with faster steam turbine start-ups even after long standstill times. HSM is realized through an electrical Trace Heating System (THS) which is placed on the outer casing and valves of the steam turbine. The benefits are shown in Figure 1, which compares start-up curves with and without HSM after standstill. Figure 1 indicates that the start-up time can be reduced by more than 60 % in HSM compared to a start-up from cold start conditions.

Furthermore, HSM offers the following advantages for steam turbine and overall power plant operation: reduced lifetime consumption of components during start-up; reduced energy share that is bypassed to the condenser; reduced fuel costs and emissions.

Alternative concepts for hot standby operation of the steam turbine rotor are known, e. g., the use of an external steam source [2] or the use of hot air [1, 3]. Both concepts require availability of auxiliary boilers and systems to provide the hot medium during plant standstill while such systems are not required in the HSM presented here.

Temperature controlling techniques have been applied in the past to small scale industrial turbines and large scale turbines with thick flanges and their main purpose is to avoid casing deformations during start-ups. The up-scaling of this technology is currently under development. Heat transfer through a steam turbine with real turbine geometry is investigated in [4]. The effect of radiation at part load on the

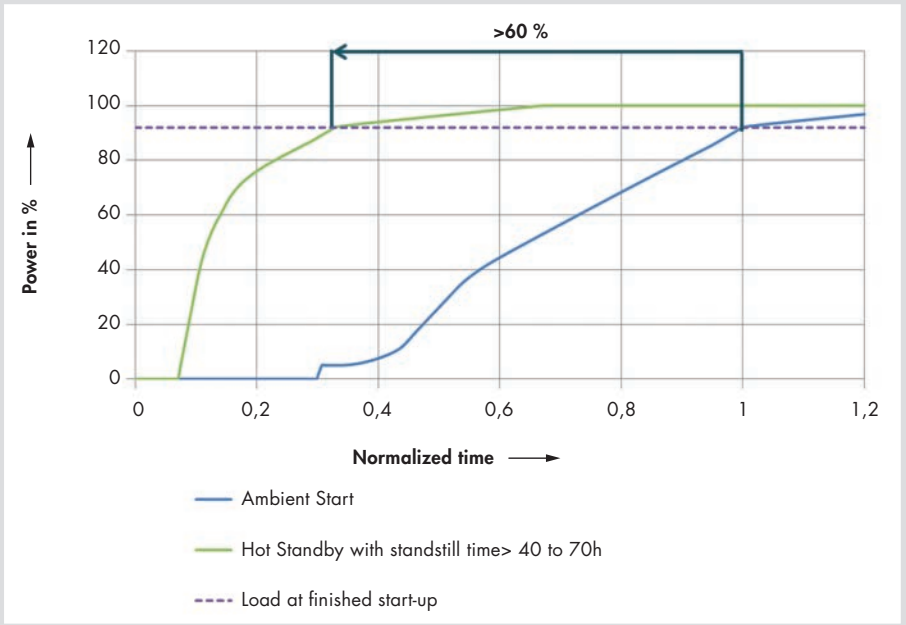

Fig. 1. Comparison of simulated start-up curves after standstill.

structural integrity was investigated by [5]. Measures to increase the flexibility of steam turbines were for example investigated by [6].

The focus of this work is to model a turbine with HSM as accurately as possible while keeping the required computational resources as low as possible. Effects of turbine geometry simplifications, which reduce computational complexity, on the accuracy of the results are examined. Modeling of the radiative heat transfer within the simplified models is specially focused on.

Hot standby mode and trace heating system

The HSM is realized by installing the THS on the steam turbine casing. The THS consists of cables such as depicted in Figure 2. In the inner conductor, electricity is transformed into heat. An insulating layer made of magnesium oxide shields the conductor from the outer sheath. The heat flux from the cables is transferred to the turbine casing and hence the turbine casing metal temperature is raised. Figure 3 shows the application of the THS on a turbine. Further information on the functionality of the THS is given in detail in [7].

Turbine geometry for testing

High (HP) and Intermediate (IP) Pressure parts of the SST-5000 steam turbine [9] are used as a model topology for investigation. A schematic of the geometry is shown in Figure 4 where important geometry is highlighted by colored lines, locations of temperature sensors for experiments are marked by red dots, and locations of sensors for the numerical HSM investigation are indicated by blue dots.

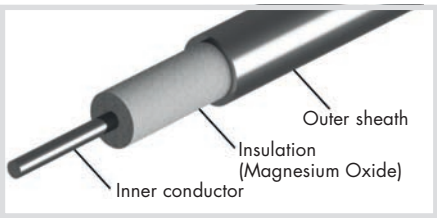

Fig. 2. Mineral insulated cable; © Thermoprozess [8]

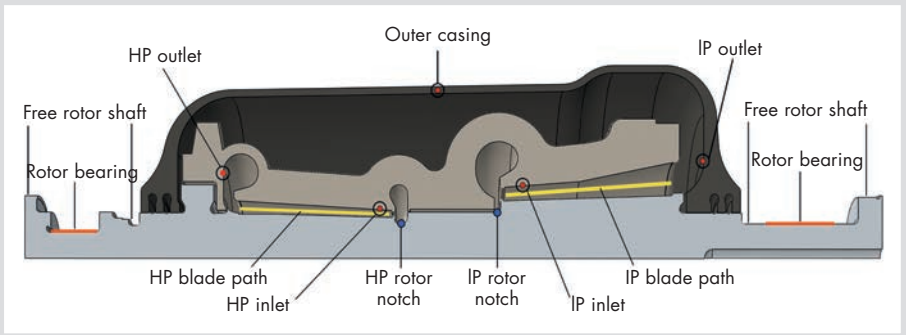

Fig. 4. Turbine model geometry including locations of temperature sensors for experimental data (red dots), temperature sensors for THS investigation (blue dots), and important geometrical aspects (red and yellow colored lines).

The cool-down of the turbine without THS has been experimentally investigated. The turbine was in full operation and then shut down while seal steam remained in operation. After a few hours the seal steam was shut off and the vacuum of the turbine broken. Temperature data was collected throughout the cool-down process at the locations marked in Figure 4. The experimental results have been employed in section 4.5 to validate the numerical models. In section 5, the experimentally investigated test case is used as a base to investigate the performance of the HSM.

Modelling the heat transfer throughout the turbine

The heat transfer throughout the turbine is investigated by simulation using Abaqus CAE. Several simplifications of the turbine geometry are used in order to reduce the computational time of the simulations. In the first model "2D model with blades" described in section 4.2, the turbine is modeled as two-dimensional. The turbine blades are represented as their projected area. In the second model, "2D model without blades" discussed in section 4.3, the turbine is modeled as two-dimensional and the turbine blades are omitted. Instead, the thermal properties of the materials are adapted to model the heat transfer accurately. The third model, "3D model without blades" discussed in section 4.4, is similar to the model of section 4.3. The turbine geometry is modeled as a symmetric quarter of the turbine without blades. Thermal properties are adapted to keep an accurate description of the heat transfer.

Heat transfer in Abaqus CAE

Heat transfer by the three mechanisms conduction, convection and radiation is accounted for in the Abaqus CAE models. The conductive heat transfer is described by

$$\dot{q}_{\mathrm{cond}} = \lambda(T)\Delta T, \tag{1}$$

where λ is the thermal conductivity, and ΔT is the temperature difference between the considered locations. The convective heat transfer is described by

$$\dot{q}_{\mathrm{conv}} = \alpha(T)\Delta T, \tag{2}$$

where α is the heat transfer coefficient. The heat transfer due to radiation is described by

$$\dot{q}_{\mathrm{rad}} = \varphi\, \varepsilon(T)\, \sigma\, T^4, \tag{3}$$

where φ is the view factor, $\varepsilon(T)$ is the emissivity, σ is the Stefan-Boltzmann constant, and T the body's absolute temperature.

Fig. 3a. HSM fixed on the outer casing of a turbine.

Fig. 3b. Insulation on turbine casing; © Thermoprozess [8].

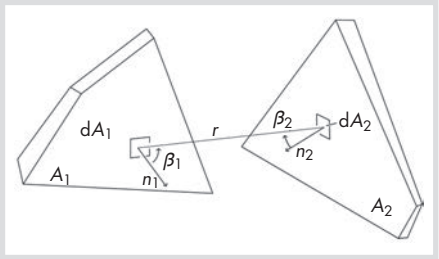

Fig. 5. Computation of view factors.

Figure 5 illustrates the computation of φ which is obtained by

$$A_i \, \varphi_{ij} = \int_{A_i} \int_{A_j} \frac{\cos \beta_i \, \cos \beta_j}{\pi \, r_{ij}^2} \, dA_i dA_j, \tag{4}$$

where the indices i and j indicated the surfaces in radiative exchange, A is the surface area, β the angle to a normal on the surface, and r the distance between the surfaces [10, 11].

In Abaqus CAE, the conductive heat transfer has been modeled using temperature dependent values of $\lambda(T)$. The convective heat transfer has been accounted for using surface film conditions with α as film coefficient and predefined sink temperatures. The value of the employed α varies linearly from inlet to outlet in the blade paths. The linear variation is chosen according the linearly varying loading profile. Radiative heat transfer is modeled using the cavity radiation model [10]. The cavity radiation employs gray body theory. The emissivity of the surfaces is independent from the wavelength of the radiation and only diffuse reflection is considered [11, 12].

2D model with turbine blades

A two-dimensional, rotationally symmetric model of the turbine is generated in Abaqus CAE. Figure 6a shows the simplified geometry. Local geometrical aspects such as flange joints, fins as well as inlets and outlets are neglected due to symmetry. The turbine blades are included as individual blades. Since the 2D model is not capable of capturing the three-dimensional shape of the blades, a projected area of the turbine blades is used as blade geometry in the model. As this method increases the total blade volume V, the density ρ_{real} is substituted according to

$$\rho_{sub} = \frac{V_{real} \, \rho_{real}}{V_{sub}}, \tag{5}$$

wherefore the correct heat capacity is restored in the model. In order to account for the effect of the change in blade cross section in the conductive heat transfer, the product of the area A and the thermal conductivity λ is kept constant in the simplified geometry. This is realized in Abaqus CAE by introducing the substitute thermal conductivity λ_{sub} computed as

$$\lambda_{sub} = \frac{A_{real} \, \lambda_{real}}{A_{sub}}. \tag{6}$$

The heat transfer of the blade root to the rotor or inner casing is modeled to include the effects of the blade root submerged in the rotor and inner casing material. The emissivity ε is chosen according to previous investigations of the material at Siemens AG.

2D model without turbine blades

The second model shown in Figure 6b is a two-dimensional model of the turbine without individually modeled turbine blades. Instead, the heat transfer from and to the turbine blades is modeled by adjusting the heat transfer parameters to account for the thermal influence of the turbine blades. The same heat flow is simulated as in the 2D model with turbine blades in section 4.2. Effects of conductive heat transfer of the blades are small compared to the convective and radiative heat transfer and are therefore neglected.

As the heat transfer by convection is directly proportional to α as shown in Eq. 2, the effect of the convective heat transfer of the turbine blades is included by changing α to a substitute thermal heat transfer coefficient α_{sub}. It is defined as

$$\alpha_{sub} = \alpha \, F_c \tag{7}$$

with

$$F_c = \frac{\dot{Q}_{conv,b}}{\dot{Q}_{conv,nb}} \tag{8}$$

where $\dot{Q}_{conv,b}$ is the heat flow when blades are geometrically considered, and $\dot{Q}_{conv,nb}$ is the heat flow when the blades are not geometrically represented. The factor F_c acts comparably to a fin efficiency [13].

Similarly, the radiative heat transfer has to be adjusted for the missing blades. In the 2D model without turbine blades, the resulting heat transfer has to be the same as for the 2D model with turbine blades. To realize this, ε has to be adjusted to ε_{sub}, taking into account the emissivities of both surfaces in radiative heat exchange as well as the effect of the new view factors without blades φ_{new}. A sensitivity analysis of the value of ε_{sub}, however, has shown that the effect of the variation of ε_{sub} is small in comparison to the effect of α_{sub}. As the computational effort of using ε_{sub} is large compared to the increase in accuracy, a constant value of ε is employed in further simulations.

A steady state simulation of the turbine in full operation is performed to generate starting temperature profiles for the cool-down process. Only heat transfer due to conduction and convection is considered during this simulation. Radiation is neglected as its effect is small in full turbine operation. This is the case due to the large convective heat transfer coefficients pre-

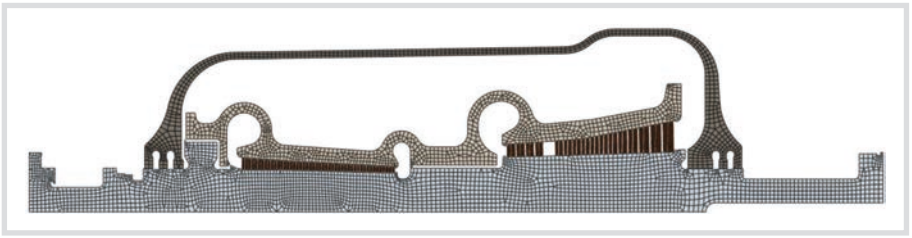

Fig. 6a. Visualization of the three models' geometries, showing the different simplifications. – 2D model with blades.

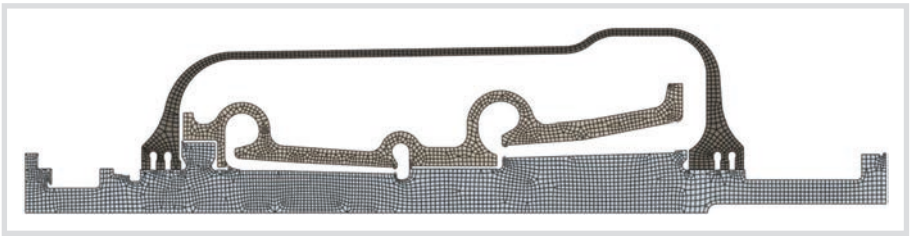

Fig. 6b. Visualization of the three models' geometries, showing the different simplifications. – 2D model without blades.

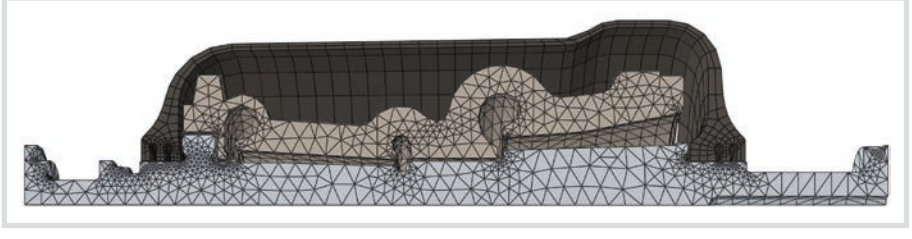

Fig. 6c. Visualization of the three models' geometries, showing the different simplifications. – 3D model without blades.

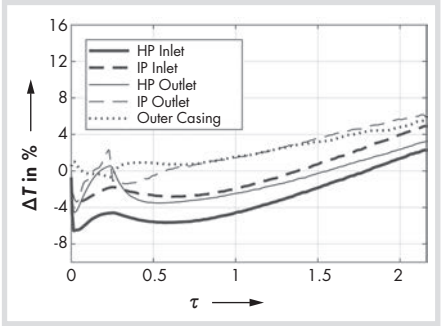

Fig. 7a. Deviation between simulated and measured temperatures normalized by the current simulated temperatures. – 2D model with turbine blades.

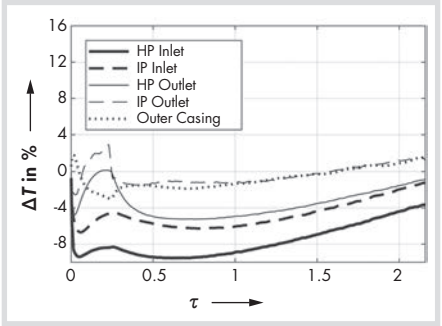

Fig. 7b. Deviation between simulated and measured temperatures normalized by the current simulated temperatures. – 2D model without turbine blades.

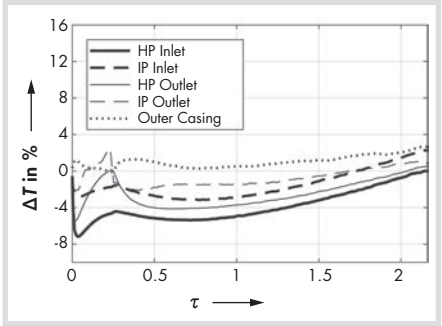

Fig. 7c. Deviation between simulated and measured temperatures normalized by the current simulated temperatures. – 3D model without turbine blades.

sent in full turbine operation. Convective boundary conditions are applied inside and outside the turbine. Inside the turbine, inlets, outlets, blade paths, and seal steam chambers are included in the convective heat transfer. Outside the turbine, the free rotor shaft, rotor bearings, and outer casing insulation are considered. In the blade paths as well as the labyrinth sealings, α_{sub} and the sink temperatures decrease linearly between the inlet and outlet to account for the pressure and velocity drops in these areas.

During the transient cool down simulation, all three heat transfer mechanisms are modeled. Convection takes place only at the turbine surfaces outside and the seal steam chambers. Heat transfer due to radiation is considered at all inner turbine surfaces with an emissivity value based on experience at Siemens AG.

3D model without turbine blades

The approach taken to model the thermal effects in the 2D model without blades in section 4.3 is used in a three-dimensional investigation. The 3D model shown in Figure 6c includes additional geometrical details at the inner casing which are not accounted for in the 2D model without blades. The 3D model is set up as a quarter model of the full steam turbine SST-5000 to reduce simulation time compared to a complete model. Similar to the 2D model without blades, no turbine blades are modeled. Boundary conditions for both the starting profile simulation and the cool-down simulation are similar to the ones of the 2D model without blades as described in section 4.3. Appropriate symmetry planes are applied to the sectional planes in the quarter 3D model for correct view factor calculations.

Validation and Comparison of the Models

The cool-down load case described in section 3 is simulated using all three models. Steady state simulations with each model generate starting conditions that match the initial temperature distribution of the experimental investigation. Transient simulations are used to capture the cool-down process.

Throughout this work, the time t is normalized to

$$\tau = \frac{t}{t_0} \tag{9}$$

which is employed in the visualization of results. The constant t_0 is the time when the rotor notch temperature first falls below a specific temperature T_t during turbine cool-down. The temperature T_t is defined to be the temperature required for fast start-up conditions.

2D Model With Blades

Figure 7a shows the deviation between the simulated and measured temperatures in the 2D model with turbine blades. The deviations at the start of prewarming are relatively large due to the simplifications in the model geometry. There are also some inaccuracies in the starting temperature conditions. Differences between the temperatures may also result from the way the experimental measurements are obtained. If the seal steam temperature is measured, this temperature might not correspond exactly to the material temperature due to conductive temperature distribution in the component and different daily boundary conditions. Deviations from experimental results decrease with time as the effects of starting conditions decline.

2D Model Without Blades

Figure 7b shows the results for the 2D model without blades. No significant differences can be observed to the results of the 2D model with turbine blades in Figure 7a. A sensitivity analysis of the effect of the thermal properties has been performed. The results show that variations of α_{sub} and ε within their range of accuracy have little effect on the overall simulation result. It is therefore sufficient to model them with the presented assumptions.

3D Model Without blades

The performance of the 3D model without blades is tested with two sets of boundary conditions. In the first simulation, the same boundary conditions as for the 2D model without blades are employed. Figure 8 shows the results. The deviations from the experimental results are large compared to the 2D model without blades despite the 3D model without blades including more geometrical detail than the 2D model without blades. Therefore, a sensitivity analysis of the convective heat transfer coefficients and temperatures at the outer casing, bearings, free rotor surface as well as α_{sub} and ε has been performed to identify the most influential boundary conditions. The largest effect on the results, which is shown in Figure 9, has the value of α at the outer casing.

Based on the sensitivity analysis, an improved set of boundary conditions (e.g.

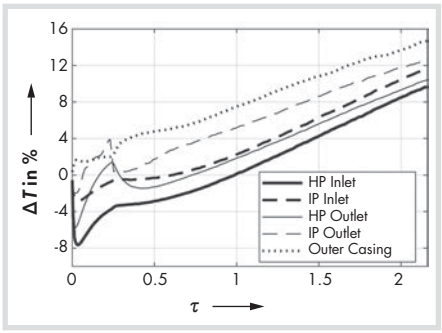

Fig. 8. Deviation between simulated and measured temperatures in the 3D model without blades normalized by the current simulated temperatures. The simulation employs the same boundary conditions as in the 2D model without blades.

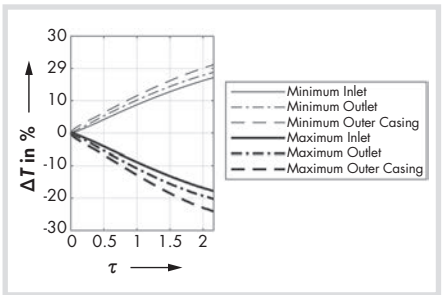

Fig. 9. Sensitivity analysis for α at the outer casing. The temperature deviations at the temperature sensor locations are shown. The temperature deviations at the HP and IP inlets and outlets are averaged.

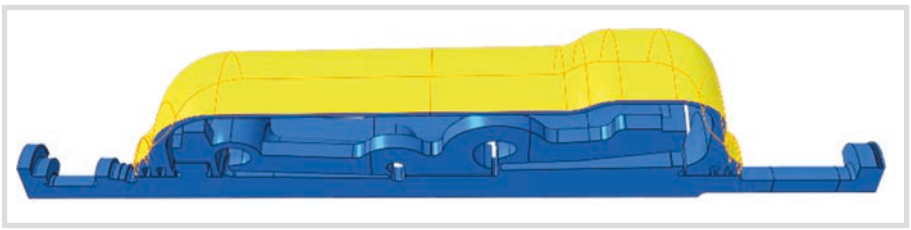

Fig. 10. Application areas of THS' heating blankets indicated in yellow.

heat transfer coefficients on outer casing) is applied in the simulation of the 3D model without blades. The adapted boundary conditions improve the results, as shown in Figure 7c. The differences between the 3D model without blades and the 2D model without blades originate on the one hand from the different boundary conditions. On the other hand, different view factors due to included flanges in the 3D model influence the results. The distances between the inner and outer casing are also smaller in the 3D model without blades a fact that influences the heat transfer. Including the flanges increases the component volume hence leading to a higher stored energy. This results in a reduced rate of cooling in the 3D model without blades.

Comparison of models

All models are able to capture the most important effects during cool down. The 3D model without blades performs better due to the more exact representation of the turbine geometry. 3D effects should not be neglected for a detailed analysis. For large scale optimization approaches, using a 2D model will be sufficiently accurate. No model is able to capture the effects at the beginning of the simulation very accurately, which is acceptable as the long term temperature distribution is the main point of interest.

Application of the HSM

The validated 3D model without blades is enhanced to additionally include the THS. The enhanced model is used to investigate the performance of the HSM.

A load case for the analysis of the warm-keeping mode is constructed based on the cool-down load case. The turbine is turned off and left to cool down. The THS is activated once the outer casing temperature reaches a threshold temperature T_t.

Different locations of the THS "heating blankets" are possible. The positioning of the heating blankets has been exemplarily investigated for the location shown in Figure 10, where the heating blanket is mounted on the whole outer casing.

The heating blankets are modeled by including their respective heat fluxes in the turbine model. The heat flux does not exceed a maximum value and the temperature of the outer casing is defined to be at maximum 5 K above T_t. A PID controller with temperature feedback loop regulates the magnitude of the heat flux. It is included via a user subroutine in Abaqus CAE. The rotor temperature is the limiting factor for warm start-up conditions and is hence chosen as the process variable. Figure 4 shows the location of the considered HP rotor notch and IP rotor notch. The analysis of the results shows that the IP rotor notch temperature is lower than the HP rotor notch temperature wherefore effectively the IP rotor notch temperature is the limiting factor.

The heat flux is the control variable u(t) for the PID controller, which is computed by [14]

$$u(t) = K_P \left[e(t) + \frac{1}{T} \int_0^t e(\tau) d\tau + T_D \frac{d}{dt} e(t) \right], \quad (10)$$

where the error value $e(t)$ is the difference between the actual and the set point temperature at the IP rotor notch.

Figure 11 shows the temperatures at the HP rotor notch and IP rotor notch. The temperatures are normalized by the starting temperature at the HP rotor notch while the time is normalized by the time of the heating blanket activation. The results show that it is possible to maintain conditions for warm start-up conditions within the turbine.

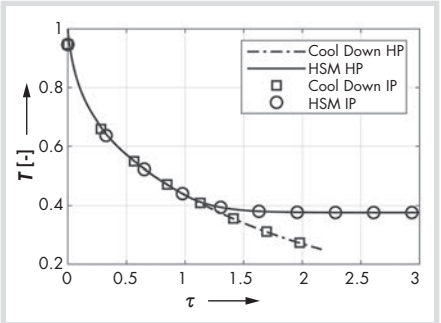

Fig. 11. Temperature profiles during cool down (Cool Down) and in warm-keeping mode (HSM) at the HP and IP rotor notches. Temperatures are normalized by the starting temperature at the high pressure notch.

Conclusions

The heat transfer throughout the complex turbine topology has been investigated using three models with different degrees of geometry simplification. The analysis shows that it is possible to capture the most important aspects using two-dimensional models with simplified topology. Further geometry simplifications can be realized by adapting the thermal behavior of the FEM-model.

A large part of the heat transfer in the turbine is realized by radiation. Without modelling this type of heat transfer, it is not possible to make an accurate prognosis of the temperature load and distribution. The simplified CAE model "2D model without blades" is able to perform the calculations faster than models with more geometrical detail. The negligible change of the accuracy, with regard to the shortening of the calculation duration, is therefore fully justifiable. A controller was further developed which makes it possible to specify the power of the HSM within the CAE simulation.

A simulation of the HSM shows that it can maintain the temperature of the turbine at a high level. The warm-keeping allows the customer to preserve the steam turbine warm start conditions without seal steam depending on their own commercial targets. As a result the energy consumption for long standstill times can be minimized.

Nomenclature

A	Area
F_c	factor for alpha substitution
$\dot{Q}$	heat flow
$\dot{q}$	specific heat flow
r	distance between surfaces
T	absolute temperature
t	time
α	heat transfer coefficient
β	angle with respect to normal to the surface
ε	emissivity
λ	thermal conductivity
ρ	density
σ	Stefan-Boltzmann constant
τ	normalized time
φ	view factor
cond	conduction
conv	convection
real	physical value
rad	radiation
sub	substitute value

References

[1] T. Eisfeld, A. Feldmüller, and F. Roehr, *"CCPP improvements in a business environment of intermittent power generation,"* in Power-Gen Europe 2017.

[2] A. Feldmüller, T. Zimmerer, and F. Roehr, *"From Base to Cycling Operation – Innovative Operational Concepts for CCPPs,"* in Power-Gen Europe 2015.

[3] D. Toebben et al., *"Numerical Investigation of the Heat Transferand Flow Phenomena in an IP Steam Turbine in Warm-Keeping Operation with Hot Air (GT2017-63555),"* Proceedings ASME Turbo Expo, 2017.

[4] H.M. Brilliant and A.K. Tolpadi, *"Analytical Approach to Steam Turbine Heat Transfer in a Combined Cycle Power Plant (GT2004-53387),"* in ASME Turbo Expo 2004.

[5] N. Lückemeyer and F. Qin, *"Mechanical Design of Large Steam Turbine Components for Part Load Conditions (GT2013-95436),"* in ASME Turbo Expo 2013.

[6] M. Topel, M. Genrup, M. Jöcker, J. Spelling, and B. Laumert, *"Operational Improvements for Startup Time Reduction in Solar Steam Turbines,"* Journal of Engineering for Gas Turbines and Power, no. 137, 2015.

[7] Y. Kostenko and D. Veltmann, *"Development of Hot Standby Mode for flexible Steam Turbine Operation (GPPS-2018-0020),"* in Proceedings of GPPS Forum 18.

[8] THERMOPROZESS Wärmebehandlung GmbH, *"http://www.thermoprozess.de,"* 2017.

[9] Siemens AG – Energy Sector, *"Siemens Steam Turbine SST-5000 Series: for combined cycle und subcritical steam applications, 2010,"* Erlangen.

[10] Dessault Systems, *Abaqus/CAE User's Guide 2014: Abaqus 6.14.*

[11] H.D. Baehr and K. Stephan, *Wärme- und Stoffübertragung: Chap. 5*, 9th ed. Berlin, Heidelberg: Springer, 2016.

[12] Dassault Systèmes, *Abaqus Theory Guide 2014: Abaqus 6.14.*

[13] F.P. Incropera, D.P. DeWitt, T.L. Bergman, and A.S. Lavine, *Principles of heat and mass transfer: Chap. 3,* 7th ed. Singapore: John Wiley & Sons, 2013.

[14] J. Lunze, *Regelungstechnik 1: Systemtheoretische Grundlagen, Analyse und Entwurf einschleifiger Regelungen: Chap. 7 and 9,* 10th ed. Berlin: Springer, 2014.

Summary

This VGB Standard VGB-S-610, "Structural Design of Cooling Towers" constitutes the joint basis – together with VGB-R 135e, "Planning of Cooling Towers", and VGB-R 612e, "Protection Measures on Reinforced Concrete Cooling Towers and Chimneys against Operational and Environmental Impacts" – for the civil engineering-related planning including design, construction and approval as well as for the construction of cooling tower facilities built from reinforced concrete. It is based on more than 50 years of experience in the construction of cooling towers gained by plant and structural design engineers, by construction companies, accredited review engineers and owners. In addition, Guideline VGB-R 613e, "Code of Practice for Life Cycle Management of Reinforced Concrete Cooling Towers at Power Plants", presents notes on in-process inspection and maintenance.

The VGB Standard was thoroughly revised and restructured compared with the last edition, VGB-R 610e of 2010, chiefly in order to increase its application and ac-ceptance by potential users outside Germany. To this end its structure was modified to make it similar to the European standards by dividing into a generally valid and internationally oriented base part and a specific national, i.e., German part. Different from the European standards, however, no national annex was created. Instead, for improved readability a unified document was produced comprising the generally applicable base part and the location-specific part (on a grey background) with German rules. For application outside Germany it is necessary to use the respective national rules and specifications instead of the German rules.

New findings from continued engineering studies and feedback from practice have also necessitated modifications. In particular, hybrid cooling towers and multi-cell cooling towers as now common cooling tower design variants have been included, in addition to natural draught cooling towers.

This VGB Standard does not cover contractual arrangements with responsibilities for organisational workflows. These are to be defined separately by the contracting par-ties. Users are requested to inform the VGB Office of their experience with the appli-cation of this VGB Standard and any sources of possible misinterpretation or short-falls in presentation, and to make suggestions for improvements. These may be tak-en as a basis for future additions or amendments.

This VGB Standard VGB-S-610e, "Structural Design of Cooling Towers", supersedes VGB Guideline VGB-R 610e of 2010 with the same name.

Special Prints / Reprints from journal VGB PowerTech

A meaningful medium, print or digital, for your technical papers
from the renown journal VGB PowerTech.

- Benefit from the image of our journal, in which only technical papers reviewed by experts are published.
- Reprints are produced individually according to your requests and with the same contents as the original paper.
- Your CI can be transferred into the paper, or you will get a copy of the original layout from our journal.

Please do not hesitate to contact us!

Mr Gregor Scharpey | phone: +49 201 8128-200 | E-mail: mark@vgb.org